AGU ADVANCING EARTH AND SPACE SCIENCE

Key Points:

- Ambiguous interspecies differences in benthic foraminiferal $\delta^{18}O$ from the Nordic Seas for the last glacial maximum are due to bioturbation
- Deep ocean temperature and $\delta^{18}O$ in central Fram Strait were ~1.5°C and 1‰ higher during the last glacial maximum
- Intermittent Nordic Seas outflow through Denmark Strait could have been the source of glacial North Atlantic water at 2–3 km water depth

Deep Ocean Storage of Heat and CO_2 in the Fram Strait, Arctic Ocean During the Last Glacial Period

Mohamed M. Ezat[1,2] , Tine L. Rasmussen[1] , Mathis P. Hain[3] , Mervyn Greaves[4] , James W. B. Rae[5] , Katarzyna Zamelczyk[1], Thomas M. Marchitto[6,7] , Sönke Szidat[8,9] , and Luke C. Skinner[4]

[1]CAGE - Centre for Arctic Gas Hydrate, Environment and Climate, Department of Geosciences, UiT, The Arctic University of Norway, Tromsø, Norway, [2]Department of Geology, Faculty of Science, Beni-Suef University, Beni-Suef, Egypt, [3]Department of Earth and Planetary Sciences, University of California, Santa Cruz, CA, USA, [4]Godwin Laboratory for Palaeoclimate Research, Department of Earth Sciences, University of Cambridge, Cambridge, UK, [5]School of Earth & Environmental Sciences, University of St. Andrews, St Andrews, UK, [6]Department of Geological Sciences, University of Colorado Boulder, Boulder, CO, USA, [7]Institute of Arctic and Alpine Research, University of Colorado Boulder, Boulder, CO, USA, [8]Department of Chemistry, Biochemistry and Pharmaceutical Sciences (DCBP), University of Bern, Bern, Switzerland, [9]Oeschger Centre for Climate Change Research (OCCR), University of Bern, Bern, Switzerland

Abstract The Fram Strait is the only deep gateway between the Arctic Ocean and the Nordic Seas and thus is a key area to study past changes in ocean circulation and the marine carbon cycle. Here, we study deep ocean temperature, $\delta^{18}O$, carbonate chemistry (i.e., carbonate ion concentration $[CO_3^{2-}]$), and nutrient content in the Fram Strait during the late glacial (35,000–19,000 years BP) and the Holocene based on benthic foraminiferal geochemistry and carbon cycle modeling. Our results indicate a thickening of Atlantic water penetrating into the northern Nordic Seas, forming a subsurface Atlantic intermediate water layer reaching to at least ~2,600 m water depth during most of the late glacial period. The recirculating Atlantic layer was characterized by relatively high $[CO_3^{2-}]$ and low $\delta^{13}C$ during the late glacial, and provides evidence for a Nordic Seas source to the glacial North Atlantic intermediate water flowing at 2,000–3,000 m water depth, most likely via the Denmark Strait. In addition, we discuss evidence for enhanced terrestrial carbon input to the Nordic Seas at ~23.5 ka. Comparing our $\delta^{13}C$ and qualitative $[CO_3^{2-}]$ records with results of carbon cycle box modeling suggests that the total terrestrial CO_2 release during this carbon input event was low, slow, or directly to the atmosphere.

1. Introduction

Late Pleistocene glaciations were characterized by millennial- and decadal-scale variations in global/regional climate and atmospheric carbon dioxide levels (i.e., pCO_2), superimposed on gradual longer-term trends of increasing ice volume and decreasing atmospheric pCO_2 (e.g., Bard et al., 1990; Barker et al., 2011; Bereiter et al., 2015; Marcott et al., 2014). For example, Greenland ice core records show that the high latitude North Atlantic region underwent ~25 millennial-scale climate oscillations during the last glacial period (~110,000–19,000 years ago; 110–19 ka), referred to as Dansgaard-Oeschger (DO) events (Dansgaard et al., 1993). These DO events, consisting of warm interstadials and cold stadials, are characterized by an abrupt atmospheric warming over Greenland of 8°C–16°C from cold stadials to warm interstadials followed by a gradual cooling and eventually a sudden cooling back to stadial conditions (Huber et al., 2006). Associated with DO events, high-resolution records of atmospheric pCO_2 from Antarctic ice cores reveal millennial-scale (up to 25 ppm) and centennial-scale (up to 10 ppm) variations (e.g., Bauska et al., 2018; Bereiter et al., 2015; Marcott et al., 2014).

The Atlantic Meridional Overturning Circulation (AMOC), which is a crucial regulator of the earth's climate variability, is thought to have played a leading role in these (sub)millennial-scale variations in climate and atmospheric pCO_2 through its control on heat redistribution and ocean-atmosphere gas exchange (e.g., Broecker, 1998; Ezat et al., 2014; Fischer et al., 2010). Modern exchange of surface and deep water between the Arctic Ocean, the Nordic Seas and the North Atlantic Ocean represents the northern limb of the AMOC (Hansen & Østerhus, 2000). Northward inflow of warm Atlantic water across the Greenland-Scotland ridge advects heat, salt and carbon to the Nordic Seas and the Arctic Ocean, where the major part of the
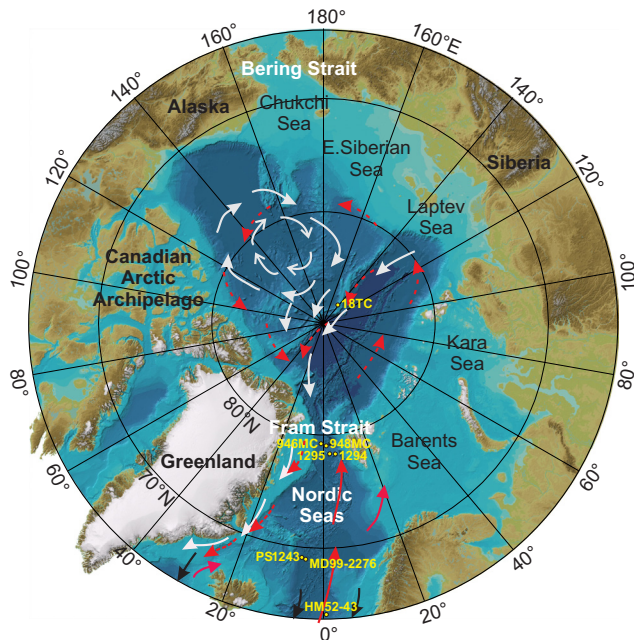
Figure 1. Map showing major ocean currents in the Nordic Seas and Arctic Ocean and the location of sediment cores. Yellow dots refer to the location of sediment cores from this study (HH12-946MC and HH12-948MC, Ezat et al., 2019) and published records discussed in this study (HLY0503-18TC, for example, Cronin et al., 2012; 1,294-4 and 1,295-5, Hebbeln et al., 1994; PS1243 and MD99-2,276, for example, Thornalley et al., 2015; HM52-43, Veum et al., 1992). Atlantic water inflow is indicated by solid red arrows (surface inflow) and dashed red arrows (submerged inflow). Freshwater circulation are shown by white arrows. Nordic Seas overflows are indicated by black arrows.

inflow water densifies and returns as deep overflows to the North Atlantic (Hansen & Østerhus, 2000). The evolution of this circulation pattern during the last glacial period and its contribution to glacial climate and atmospheric pCO_2 variations is still elusive. For example, deep ocean exchanges between the Arctic Ocean and the Nordic Seas are particularly poorly constrained during the Last Glacial Maximum (LGM; 25–19 ka), when global ice sheets reached their maximum integrated volume (e.g., Clark et al., 2009). Moreover, carbon exchanges between the deep ocean, the surface ocean and the atmosphere are even less constrained in the Arctic Ocean and Nordic Seas for the last glacial period. This is partly due to limited availability of deep-sea sediments dating from the LGM from the central Arctic Ocean, because of extensive sea ice cover resulting in very low or no sedimentation (e.g., Hanslik et al., 2010). In addition, $\delta^{18}O$ values measured in benthic foraminifera from the deep northern and central Nordic Seas show large and ambiguous interspecies differences (Bauch et al., 2001; Ezat et al., 2019).

The Fram Strait is an important gateway between the Arctic Ocean and the Nordic Seas and thus is a key area to investigate the heat and carbon exchanges between the Arctic Ocean, the Nordic Seas and the Atlantic Ocean. In addition, marine records from the deep Fram Strait document enhanced flux of terrestrial carbon to the northern Nordic Seas at ~24 ka (Hebbeln et al., 1994). Changes in terrestrial carbon storage have also been suggested to have played a role in some abrupt centennial-scale changes in atmospheric pCO_2 (e.g., Bauska et al., 2016). Given the vast and dynamic permafrost and subglacial carbon reservoirs in the Arctic region (e.g., Köhler et al., 2014; Meyer, Hefter, Köhler, Tiedemann, Gersonde, Wacker, Mollenhauer et al., 2019; Tarnocai et al., 2009; Vonk et al., 2012; Wadham et al., 2019), and the increased melting and release of huge icebergs from surrounding ice sheets (e.g., Bjørk et al., 2012; Luckman et al., 2006; Mankoff et al., 2020), it is imperative to study the impact of a possible "terrestrial carbon mobilization" event at ~24 ka on deep ocean carbonate chemistry and atmospheric pCO_2.

Here, we assess the interspecies differences in benthic foraminiferal $\delta^{18}O$ and study the glacial evolution of deep-ocean temperatures, $\delta^{18}O$ and carbonate chemistry in the deep, central Fram Strait (~2,600 m water depth) for the 35–19 ka period using benthic foraminiferal element/Ca, radiocarbon and isotope measurements from two deep ocean sediment cores (~2,600 m water depth). In addition, we use the CYCLOPS carbon cycle box model to assess the effects of a possible "terrestrial carbon mobilization" event at ~24 ka on atmospheric pCO_2 and the carbonate chemistry of the deep "Northern Component Water", and compare the model results with our proxy reconstructions. The overall purpose is to study the exchange of deep water through the Fram Strait and explore the contribution of ocean circulation and biogeochemical changes in the northern Nordic Seas to glacial climate and carbon cycle variations.

2. Material and Methods

This study is based on new and published data from two sediment cores HH12-946MC (78°53'N; 01°45'W; 2,637 m water depth) and HH12-948MC (78°52'N; 00°21'E; 2,542 m water depth) from the central Fram Strait (Ezat et al., 2019, Figure 1). Published results from sediment cores HLY0503-18TC (88°45'N; 146°68'E; 2,654 m water depth; Cronin et al., 2012), PS1243 and MD99-2,276 (69°37'N, 06°55'W, 2,711 m water depth; Bauch et al., 2001; Thornalley et al., 2015), 1,294-4 (77°59.9'N; 5°22.3'E; 2,668 m water depth; Hebbeln et al., 1994), 1,295-5 (77°59.2'N; 2°24.8'E; 3,112 m water depth; Hebbeln et al., 1994), and HM52-43 (64°25'N, 0.73°E, 2,781 m water depth; Veum et al., 1992) are also closely compared and discussed (Figure 1).

2.1. Stable Carbon and Oxygen Isotopes

We use published foraminiferal $\delta^{18}O$ and $\delta^{13}C$ records of the planktic species *Neogloboquadrina pachyderma*, the shallow infaunal benthic species *Oridorsalis umbonatus* and the epifaunal benthic species *Cibicidoides wuellerstorfi* from cores HH12-946MC and HH12-948MC (Ezat et al., 2019). In order to increase the temporal resolution and extend the investigated time interval, new measurements were obtained on *O. umbonatus* following the methods described in Ezat et al. (2019).

In addition, new stable isotope measurements on *C. wuellerstorfi* from core HH12-948MC were made after acid leaching. About 6 specimens of *C. wuellerstorfi* were crushed and leached by 0.01M HCl for 15 min, including ultrasonication for 5 min. Thereafter, the samples were rinsed immediately by milliQ water. The $\delta^{18}O$ and $\delta^{13}C$ were then measured at the Godwin Laboratory for Paleoclimate Research, University of Cambridge, UK. These new measurements were performed to investigate the possibility that the low $\delta^{18}O$ previously recorded in *C. wuellerstorfi* (Bauch et al., 2001; Ezat et al., 2019; Thornalley et al., 2015) could be caused by diagenetic coating with extremely low $\delta^{18}O$. It was not possible to perform this "acid leaching" test on core HH12-946MC, because all specimens of *C. wuellerstorfi* in this core were already used for stable isotope analyses and radiocarbon dating (see below).

2.2. Benthic Element/Ca Analyses and Seawater Temperature and $\delta^{18}O_{water}$ Calculations

For element/Ca analyses, we used the most persistent and abundant benthic foraminiferal species in our study region, *O. umbonatus* (Bauch et al., 2001; Ezat et al., 2019). A total of 25–30 pristine specimens of *O. umbonatus* were carefully picked from the 150–250 µm size fraction from sediment cores HH12-948MC and HH12-946MC. After crushing, the samples were cleaned following the reductive-oxidative method described in Pena et al. (2005) and originally published in Boyle and Keigwin (1985). At the day of analyses, the samples were dissolved using 330 µl 0.1M HNO_3. After centrifugation for 5 min (7,000 rpc), 300 µl of the samples were transferred to new acid-cleaned vials. For blank samples (which have been treated with cleaning reagents as actual samples), 50 µl of a high purity 2,000 ppm Ca^{2+} solution was added before adding the acid, to enable determination of the blanks as element/Ca. An aliquot of 50 µl of each sample was added to 200 µl 0.1M HNO_3 and analyzed on an ICP-OES to determine their $[Ca^{2+}]$. Accordingly, the samples were re-diluted to 10 ppm $[Ca^{2+}]$ using "0.3M HF - 0.1M HNO_3" mixture and were analyzed by HR-ICP-MS at the University of Cambridge following Misra et al. (2014). Based on repeated measurements of in-house standard solutions ($n = 11$), the analytical precision (2 sd) for both B/Ca and Mg/Ca is 0.9%. Blank samples ($n = 9$) show average B/Ca and Mg/Ca of 2.5 µmol/mol and 0.027 mmol/mol, respectively, suggesting insignificant contamination from vials or cleaning/dissolution reagents. Mn/Ca, Fe/Ca (except two samples) and Al/Ca (except four samples) are <25 µmol/mol, 50 µmol/mol and 50 µmol/mol respectively, indicating negligible contamination by terrigenous materials or diagenetic coatings (e.g., Barker et al., 2005).

Mg/Ca was converted to bottom water temperature (BWT; °C) using the equation from Barrientos et al. (2018) (*O. umbonatus* Mg/Ca = A * exp (0.102 ± 0.01 * BWT). The pre-exponential constant (A) is calibrated to our core-top samples from core HH12-948MC (which are <2,000 years BP) yielding a value of 1.45. Elderfield et al. (2006) has shown that Mg/Ca data of *O. umbonatus* from sites with BWT <2°C do not follow a simple calibration curve. This could be related to the "carbonate ion" effect (e.g., Elderfield et al., 2006), partial dissolution, and/or use of a wide size range of foraminiferal specimens (e.g., Tisserand et al., 2013). Nevertheless, the consistency between published BWT reconstructions based on Mg/Ca measurements of *O. umbonatus* and independent BWT reconstructions from clumped isotopes (Thornalley et al., 2015) and Mg/Ca measured on ostracods (Cronin et al., 2012) from the central Nordic Seas (see Thornalley et al., 2015) provides confidence in the use of this species in BWT reconstructions in our study region.

Seawater $\delta^{18}O$ was calculated by removing the temperature component of the $\delta^{18}O$-*O. umbonatus* using the equation from Shackleton (1974). To convert from the Pee Dee Belemnite scale for carbonate $\delta^{18}O$ to Standard Mean Ocean Water for $\delta^{18}O$-water, 0.2 was added (Shackleton, 1974). Using other available equations (Bemis et al., 1998; Marchitto et al., 2014) would change the amplitude of glacial-interglacial change in seawater $\delta^{18}O$ by <0.1‰.

Table 1
Radiocarbon Dates on Neogloboquadrina Pachyderma, Cibicidoides Wuellerstorfi and Oridorsalis Umbonatus From Core HH12-946MC

Sediment depth (cm)	Calendar age (ka)	^{14}C age (years BP)		
		N. pachyderma	*C. wuellerstorfi*	*O. umbonatus*
25.25	19.7	18,075 ± 90		18,580 ± 88
25.75	20.1	18,399 ± 75		18,511 ± 82
27.25	20.6	18,765 ± 73	14,460 ± 190	18,787 ± 95
28.25	21.2	19,335 ± 77	14,206 ± 205	19,232 ± 148
29.25	22.6	19,833 ± 284	15,175 ± 169	
29.75	23.3		15,372 ± 205	
30.75	24.7	22,372 ± 108		
32.75	25.5	23,076 ± 131		25,327 ± 161
33.75	27.1	24,741 ± 134		26,118 ± 170
35.75	30.7	28,333 ± 225		29,715 ± 340

Note. Gray-highlighting indicates samples measured by "gas source-based techniques" (this study; see Methods), while other samples were measured by "graphitization-based" methodology (Ezat et al., 2019).

2.3. Radiocarbon Analyses

Four ^{14}C dates from core HH12-946MC on specimens of *C. wuellerstorfi* (~250–600 µg carbonate per sample) were measured following Gottschalk et al. (2018) using the Mini Carbon Dating System (MICADAS) at the University of Bern (Szidat et al., 2014). In brief, foraminiferal samples were loaded into septum-sealed glass vials. The air in the vials was removed and replaced by He using two concentric needles inserted through the septum by the automated carbonate handling system. The foraminiferal samples were then weakly leached by adding 200 µl 0.01 M HCl for 3 min at room temperature. After a second flush of the vials with He (to remove CO_2 produced during leaching), 0.5 mL 85% (~15 M) orthophosphoric acid (H_3PO_4) was added with a gas-tight syringe for carbonate dissolution. The reaction was run to completion over night at a temperature of 70°C. To evaluate possible methodological bias when comparing between "MICADAS-based" *C. wuellerstorfi* and published "graphitization-based" *O. umbonatus* and *N. pachyderma* ^{14}C dates measured at the ^{14}Chrono Center, Queen's University Belfast, Northern Ireland (Ezat et al., 2019), one *N. pachyderma* ^{14}C date was measured by MICADAS following the methods outlined above. The MICADAS-based *N. pachyderma* date is consistent with "graphitization-based" *N. pachyderma* dates (Table 1; Figure S1), indicating negligible methodological bias.

2.4. Age Models

The age models of cores HH12-946MC and HH12-948MC have been published previously (Ezat et al., 2019) and are based on calibrated planktic 14C dates (Tables S2 and S3) using the Marine13 data set in Calib 7.04 (Reimer et al., 2013). Here we update the age models using the recently published Marine20 data set (Heaton et al., 2020) in Calib 8.2 (Stuiver et al., 2020) (Tables S1 and S2). We used ΔR (the regional difference from the average global marine reservoir correction) = 1,000 years (i.e., reservoir age = ~1,500 years) for the glacial parts of the records and ΔR = 0 for the Holocene. Although changes in the reservoir age in the Fram Strait during the last glacial period remain unconstrained, the assigned value of 1,500 ^{14}C years are consistent with reservoir age estimates from the southern and central Norwegian Sea (Ezat et al., 2017; Thornalley et al., 2015) as well as with modeling results (e.g., Butzin et al., 2020). The resulting sedimentation rates range from 0.6 to 9 cm/kyr in core HH12-946MC, with an average of 2 cm/kyr for both the Holocene and glacial parts (Tables S1 and S2). These relatively low sedimentation rates can potentially induce large smoothing effects from bioturbation. However, because the ^{14}C dates of *N. pachyderma* and *O. umbonatus* are in chronological for the glacial part of the record, and because ^{14}C dates of *O. umbonatus* are older than those of *N. pachyderma* (except for one sample at 28.25 cm, but the difference is less than the analytical uncertainty; Table 1), we conclude that the impact of burrowing activity is minor. Furthermore, our study mainly target the relatively long-term changes from late MIS 3 to LGM. According to the age model, the transition from late MIS3 to the LGM is characterized by a pronounced increase in δ^{18}O values measured in *N. pachyderma* and *O. umbonatus* (Ezat et al., 2019; see also "Results and Discussion" section), which provides confidence in our age model at such timescales.

The original age models of sediment cores 1,294, 1,295 from the eastern Fram Strait were based on uncorrected planktic radiocarbon dates (Hebbeln et al., 1994). We updated the original age models of cores 1,294, 1,295 by the same approach as for cores HH12-946MC and HH12-948MC (Tables S3 and S4). The age models of sediment cores PS1243 and MD99-2,276 from the central Nordic Seas were based on correlation to the well-dated sediment cores from the southern Norwegian Sea (see Rasmussen & Thomsen, 2004) using the planktic δ^{18}O (Ezat et al., 2017; Thornalley et al., 2015). Unfortunately, because of missing data from the deglaciation, the planktic δ^{18}O records from the Fram Strait cannot be correlated with the records from the southern Norwegian Sea. Finally, in this study, we define a Heinrich stadial as the whole stadial period during which a Heinrich event occurred (e.g., Barker et al., 2011).

2.5. Carbon Cycle Modeling

Given the evidence of an abrupt +10 ppm jump in atmospheric CO_2 (e.g., Ahn & Brook, 2014; Bereiter et al., 2015) and an enhanced influx of terrestrial carbon to the Nordic Seas (Hebbeln et al., 1994) at the Heinrich Stadial 2/Interstadial 2 transition (~23.5 ka), we are interested if and how the "mobilization of terrestrial carbon" could be recorded in "Northern Component Water". For this, we used the glacial configuration of the CYCLOPS carbon cycle box model (Hain et al., 2010, 2014) as a point of comparison to our observational records and in order to assess the effects of possible mobilization of terrestrial carbon at this time. The baseline model scenario is spun-up to the reference LGM conditions, including Southern Ocean changes that dominated simulated glacial CO_2 drawdown (Hain et al., 2010; Sigman et al., 2010), as well as a "Glacial North Atlantic Intermediate Water" (GNAIW; e.g., Lynch-Stieglitz et al., 2007) representation of the AMOC that is, needed to account for the gross pattern of LGM and deglacial carbon isotope changes (Hain et al., 2014; Sigman et al., 2003). The GNAIW configuration in CYCLOPS has the same 21.5 Sv strength (1 Sv = 10^6 m^3/s) as the default NADW configuration, but the lower limb of the southward return flow is restricted to middepth as opposed to present-day NADW flowing in the deep Atlantic basin. This initial steady state of the model is perturbed with a sequence of Atlantic circulation changes that is, designed to mimic the Heinrich stadial 2/interstadial 2 transition changes; starting with GNAIW, switching to a "Heinrich Stadial" collapsed state of the AMOC for the duration of Heinrich stadial 2 (4,000 years), followed by the default NADW circulation to represent vigorous and deep overturning during interstadial 2 (1,300 years), and finally a return to the initial GNAIW circulation. This treatment is equivalent to the representation of the deglacial AMOC changes described in Hain et al. (2014). Assuming these simplistic "ad hoc" changes adequately reflect Atlantic changes over the Heinrich stadial 2/interstadial 2 interval, the simulated biogeochemical changes in the "Northern Component Water" model reservoir, which represents the subsurface high-latitude North Atlantic including the Nordic Seas, serve as a comparison baseline for our observational data. To simulate the spectrum of hypotheses of how terrestrial carbon may have been mobilized from the largely glaciated high-northern continents we consider both (a) oxidation on land with CO_2 release directly to the atmosphere, and (b) erosion and transfer of terrestrial carbon to the deep Nordic Seas/Arctic Ocean (as represented by the "Northern Component Water"). In each of these two pathway cases, we simulate 100-year mobilization events incrementing the total amount of carbon released from zero to 88 Pg C (1 Pg C = 10^{15} gram carbon), similar to the experiments of Köhler et al. (2011, 2014) where 125 Pg C from land was released to the atmosphere at 14.6 ka within a time window of 50–200 years. In this paper, we only discuss the results from the carbon addition experiments. For a summary of the results from idealized circulation scenarios, see Supporting Information Text S1.

3. Results and Discussion

3.1. Interspecies Benthic Foraminiferal δ^{18}O Differences and Implications

One significant obstacle to reconstruct deep ocean conditions in the northern and central Nordic Seas for the last glacial period is the ambiguous large δ^{18}O differences between the epifaunal benthic foraminiferal species *C. wuellerstorfi* and the shallow infaunal species *O. umbonatus* (Bauch et al., 2001; Ezat et al., 2019; Thornalley et al., 2015). Epifaunal δ^{18}O is ~1‰ lower than coeval infaunal δ^{18}O from sediments dated to the LGM (Figure 2). In addition, the epifaunal δ^{18}O from the LGM sediments is up to 1‰ lower compared to the Holocene, which is in contrast to all other ocean basins and the SE Norwegian Sea (Figure 2). It has been suggested that this low epifaunal δ^{18}O from the LGM sediments indicates short-term, but regional ventilation events by brine formation (Bauch et al., 2001). However, it remains possible that *C. wuellerstorfi* specimens were transported from younger/shallower sediments or have a diagenetic carbonate coating with very low δ^{18}O. Our results show that intensive acid leaching before δ^{18}O measurements (see Methods) did not change the δ^{18}O values (Figure 2d). Thus, we can here eliminate the possibility that the low *C. wuellerstorfi* δ^{18}O values are due inorganic carbonate coatings.

Radiocarbon dating of *C. wuellerstorfi* could reveal whether these *C. wuellerstorfi* specimens are autochthonous. The abundance of *C. wuellerstorfi* in the glacial sediments from the central and northern Nordic Seas is very low (~<5% of the benthic foraminiferal assemblages compared to 40% during the Holocene) with an average of 7 specimens per sample (~300 μg carbonate) (Bauch et al., 2001; Ezat et al., 2019).
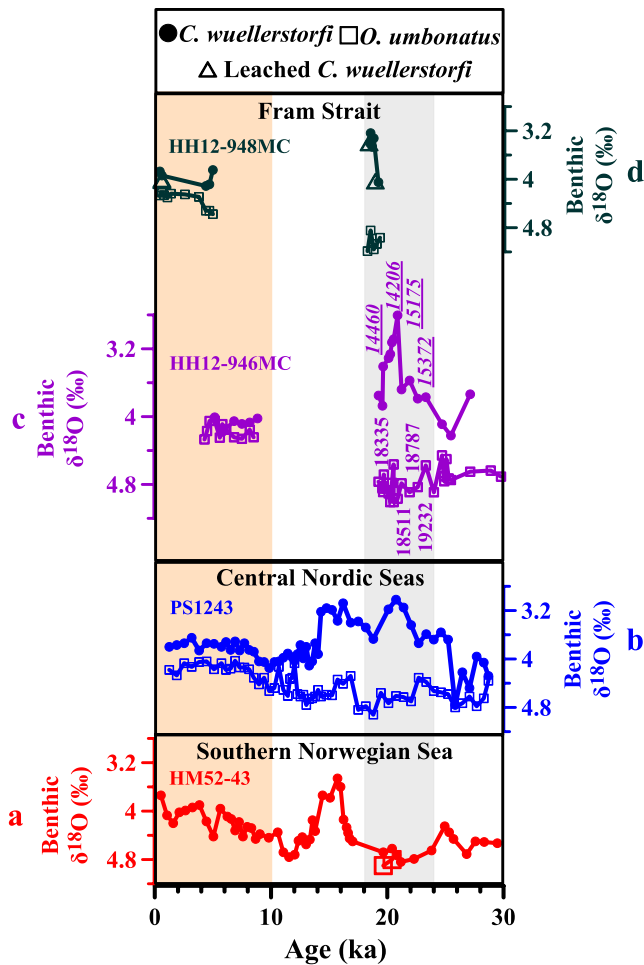
Figure 2. Benthic δ18O records from the Nordic Seas. Southern Norwegian Sea (red curve; Veum et al., 1992), central Nordic Seas (blue curves; Bauch et al., 2001) and Fram Strait records HH12-946MC (purple curves), HH12-948MC (black curves) (Ezat et al., 2019; this study). Numbers in plot (c) are un-calibrated 14C dates obtained on *C. wuellerstorfi* (italic, underlined font) and *O. umbonatus* (normal font). Triangles in (d) shows δ18O in *C. wuellerstorfi* after extensive acid leaching. Gray and orange highlighting refer to the Last Glacial Maximum (LGM) and the Holocene, respectively.

Our MICADAS 14C dates, obtained on small samples of *C. wuellerstorfi* from the LGM sediments, range from 14,000 to 15,400 14C years BP. Furthermore, they date ~4,500 14C years younger than the ages obtained on coeval *O. umbonatus* and *N. pachyderma* (Figures 2c and Table 1). This clearly indicates that these *C. wuellerstorfi* specimens are not of LGM age and that the specimens probably have been reworked from younger sediments. These results confirm that caution is needed when using low abundant "proxy carriers" from low sedimentation rate areas (cf., Peng & Broecker, 1984). However we also note that down-mixing of Holocene specimens cannot fully explain the young ages of *C. wuellerstorfi* because δ18O values in *C. wuellerstorfi* from the LGM sediments are even lower than those from the Holocene. The deglacial sediments in our two records from the central Fram strait are barren of calcareous foraminifera, which have been attributed to either post-depositional dissolution or unfavorable conditions (Ezat et al., 2019; Zamelczyk et al., 2014). If post-depositional dissolution was the reason for the absence of foraminifera in the deglacial sections of our Fram Strait cores, an earlier downcore mixing of deglacial foraminifera with very low δ18O (typical of HS1 in this region) into the LGM sediments may have occurred. However, we emphasize that the reworking process of *C. wuellerstorfi* into the LGM sediments remains not fully explained.

Regardless of the transport mechanism of younger *C. wuellerstorfi* into the LGM sediments in the deep Fram Strait, it is clear that the geochemical signals in *C. wuellerstorfi* (e.g., δ18O and δ13C) cannot be used in this context to infer hydrographic and ventilation changes in the region during the LGM. Given the striking similarity of δ18O measured in *C. wuellerstorfi* from LGM sediments in the Fram Strait (Ezat et al., 2019; this study) and the central Nordic Seas (Bauch et al., 2001) (Figure 2), our results suggest that inferences of the ocean circulation during the LGM based on δ18O and δ13C in *C. wuellerstorfi* from the central Nordic Seas (e.g., Bauch et al., 2001; Knies et al., 2018; Mackensen & Schmiedl, 2019; Thornalley et al., 2015) also should be treated with caution. Radiocarbon dating of the *C. wuellerstorfi* from the central Nordic Seas could settle the issue about reworking. We thus base our reconstructions of ocean circulation and carbonate chemistry in the northern Nordic Seas on shell geochemistry of *O. umbonatus*.

It is also notable that δ18O of *C. wuellerstorfi* from the deep southern Norwegian Seas do not show the same low values for the LGM and that δ18O values of both *C. wuellerstorfi* and *O. umbonatus* are consistently high (Veum et al., 1992) (Figure 2b) similar to *O. umbonatus* δ18O from the central and northern Nordic Seas (Figure 2). This provides confidence in using *C. wuellerstorfi* geochemistry from LGM sediments from the southern Norwegian Sea records, in contrast to the northern (and likely central) Nordic Seas deep records.

3.2. Deep Temperature and δ18O Evolution

Our BWT reconstructions from ~2,600 m water depth from the central Fram Strait based on Mg/Ca in *O. umbonatus* varies between −0.2°C and 1°C during MIS 3 (~40–26 ka) with an average of 0.6°C ± 0.5°C (Figure 3b). This is ~1.5°C ± 0.5°C warmer than the modern and average Holocene temperatures, which are ~−0.8°C (Figure 3b). These BWT changes are in agreement with those from the central Arctic Ocean at the same water depth based on Mg/Ca in ostracods (Cronin et al., 2012) (Figure 3). Our BWT record further shows an increasing trend along the transition from MIS 3 to the LGM with the highest BWT (~1.2°C) recorded at ~26–24 ka (Figure 3b). At ~23.5 ka, close to the timing of interstadial 2, the BWT decreased to ~0°C and thereafter it fluctuated between ~0°C and 0.5°C at 22–20 ka (Figure 3b).
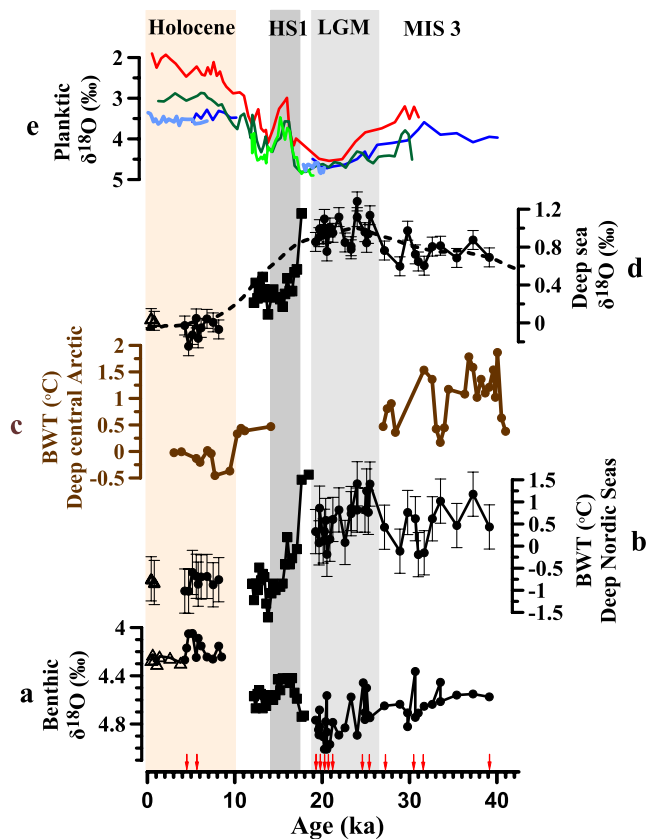
Figure 3. Deep Fram Strait, central Nordic Seas and Arctic Ocean temperature and $\delta^{18}O$ during the last glacial period. (a) $\delta^{18}O$ in *O. umbonatus* from Fram Strait records HH12-946MC (circles; Ezat et al., 2019; this study), HH12-948MC (triangles; Ezat et al., 2019) and Central Nordic Seas core MD99-2,276 (squares; Thornalley et al., 2015). (b) Deep ocean temperature based on Mg/Ca in *O. umbonatus* from cores core MD99-2,276 (squares; Thornalley et al., 2015), HH12-946MC (circles) andHH12-948MC (triangles). Error bars represent the combined "analytical" (based on 2 s.d. of replicate measurements of in-house standard) and "calibration" uncertainties. (c) Deep ocean temperature based on Mg/Ca in ostracods from the central Arctic Ocean, core HLY0503-18TC (Cronin et al., 2012). (d) Seawater $\delta^{18}O$ based on Mg/Ca and $\delta^{18}O$ in *O. umbonatus* from cores HH12-946MC (circles, this study), HH12-948MC (triangles, this study) and core MD99-2,276 (squares, Thornalley et al., 2015). Dashed line represents average global ocean $\delta^{18}O$ following Spratt and Lisiecki (2016). (e) Planktic $\delta^{18}O$ records from the southern Norwegian Sea (red, core HM52-43, Veum et al., 1992), central Nordic Seas (dark green, core PS1243, Bauch et al., 2001; green, core MD99-2,276, Thornalley et al., 2015), and Fram Strait (blue, HH12-946MC; light blue, HH12-948MC; Ezat et al., 2019 and this study). Red arrows above the *x*-axis refer to the location of the calibrated planktic 14C dates that have been used in the age model of core HH12-946MC.

Deep benthic foraminiferal $\delta^{18}O$ records from the Nordic Seas (excluding epifaunal records from the central and northern Nordic Seas; see Section 3.1) reveal a glacial-interglacial change of only 0.7‰ (Figures 2 and 3a), which is smaller than records from other ocean basins. Our deep-water $\delta^{18}O$ estimates based on $\delta^{18}O$ and temperature correction using Mg/Ca in *O. umbonatus* shows a 1‰ glacial-interglacial change, which is similar to the estimated global average ocean $\delta^{18}O$ change (Figure 3d). Seawater $\delta^{18}O$ in the deep Nordic Seas increased from 0.7‰ during late MIS 3 to 1‰ during the LGM (Figure 3d). This pattern mimics the global ocean changes in deep-water $\delta^{18}O$ (Figure 3d). The consistent amplitude and evolution of seawater $\delta^{18}O$ variations in the Nordic Seas (and possibly the central Arctic Ocean) and the mean global ocean change are in agreement with persistent exchange of deep water with other ocean basins (though likely with different modes and rates) and argue against extreme isolation of the Arctic Ocean. This is consistent with the new ^{14}C-based evidence from the Fram Strait (Ezat et al., 2019). Based on the previously inferred 'stagnation' of the deep Arctic Ocean and the Nordic Seas (ventilation ages up to 10,000 years), geothermal heating was suggested as a significant contributor to the glacial deep ocean warming in the region (Thornalley et al., 2015). In contrast, recent ^{14}C evidence from the Fram Strait (Ezat et al., 2019) and our deep-water $\delta^{18}O$ evolution (Figure 3d) suggest smaller ventilation ages and more exchange with other ocean basins, which would have limited the contribution of geothermal heating to the deep-water warming. We propose that these observations can be reconciled if the glacial warming observed in the Nordic Seas is attributed instead to thickening and/or deepening of the Atlantic intermediate water, allowing it to influence deeper areas than at present. This also suggests a significant reduction and/or shoaling of cold deep water formation by open ocean convection. Planktic $\delta^{18}O$ records from the Nordic Seas display an increase from the southern Norwegian Sea (64° 25N), central Nordic Seas (69°37′N) to the Fram Strait (78°53′N) during the Holocene (Figure 3e), which likely reflects the cooling of the Atlantic water as it flows northward. This gradient is largely diminished during the glacial period in particular at 22–19 ka (Figure 3) probably suggesting overall colder sea surface temperatures in the region and a dominant subsurface flow (and thus negligible heat loss) instead of a surface flow subject to air-sea exchange.

3.3. Carbonate Chemistry and $\delta^{13}C$ Records

Epifaunal benthic foraminiferal geochemistry is typically used to reconstruct deep ocean chemistry changes (e.g., Duplessy et al., 1988; Mackensen & Schmiedl, 2019; Yu & Elderfield, 2007). Given the reworking problem that we identify with the available epifaunal species (*C. wullerstorfi*) from the glacial sediments in our study area (see Section 3.1), we instead use $\delta^{13}C$ and B/Ca measured in the shallow infaunal benthic foraminiferal species *O. umbonatus* for the reconstruction of carbonate chemistry changes. In the North Atlantic Ocean, *O. umbonatus* lives in the upper 1 cm of the sediments (Corliss, 1985), which may indicate influence from pore water chemistry. However, the overall low productivity and supply of carbon to the deep sea as well as low sediment accumulation rates in the Fram Strait likely suggest insignificant decoupling between bottom water and shallow (<2 cm deep in the sediments) pore water chemistry. In addition, the central Arctic Ocean equivalent of *O. umbonatus* (*O. tener*) is considered to have an epifaunal microhabitat (Barrientos et al., 2018; Murray, 2006). In general, B/Ca in benthic foraminifera, including infaunal species, show a positive correlation with the
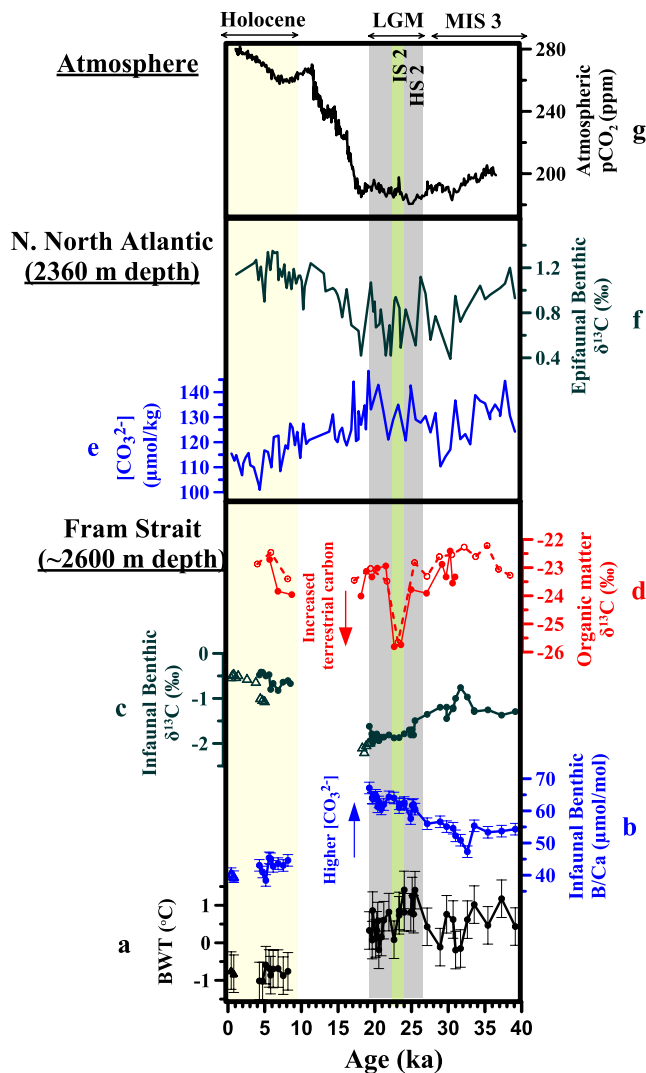
Figure 4. Evolution of deep ocean chemistry in Fram Strait and subpolar North Atlantic Ocean. (a) Deep ocean temperature from Fram Strait records HH12-946MC (circles), HH12-948MC (triangles). (b) B/Ca in *O. umbonatus* from cores HH12-946MC (circles) and HH12-948MC (triangles). Errors bars are based on 2 s. e. of replicate measurements of in-house standard (see Methods). (c) δ^{13}C in *O. umbonatus* from cores HH12-946MC (circles) and HH12-948MC (triangles). (d) δ^{13}C in organic matter from the Fram Strait records 1,295-5 (dashed line and open circles) and 1,294-4 (solid line and filled circles) (Hebbeln et al., 1994). (e) Carbonate ion concentration based on B/Ca measured in from core NEAP 8K (Yu et al., 2008). (f) δ^{13}C measured in *C. wuellerstorfi* from core NEAP 8K (Yu et al., 2008). (g) Atmospheric pCO_2 from Antarctic ice cores (Bereiter et al., 2015 and references therein).

deep-water carbonate saturation ($\Delta[CO_3^{2-}]$), providing a method for the reconstruction of deep-ocean carbonate ion concentration ([CO_3^{2-}]) (Rae et al., 2011; Yu & Elderfield, 2007; Yu et al., 2008). Carbonate ion concentration broadly records the difference or ratio between the two master variables of the carbonate system, Alkalinity and Dissolved Inorganic Carbon (DIC), allowing [CO_3^{2-}] reconstructions to inform on past changes in carbon storage in the ocean (Broecker & Peng, 1982; Yu et al., 2008, 2016). Thus, we use *O. umbonatus* B/Ca and δ^{13}C as qualitative indicators of [CO_3^{2-}] and nutrients, respectively. Given the shallow infaunal habitat of *O. umbonatus*, this should nonetheless be taken with caution.

The B/Ca in *O. umbonatus* increased from ~52 μmol/mol during late MIS 3–~62 μmol/mol during the LGM and subsequently decreased to ~43 μmol/mol during the Holocene (Figure 4b). This suggests higher glacial [CO_3^{2-}], with highest values during the LGM as seen in many studies for middepth records from the North Atlantic Ocean (Yu et al., 2008, 2010, 2020). The δ^{13}C in the infaunal species *O. umbonatus* is on average ~1‰ lower during the last glacial (~40–19 ka) compared to the Holocene (Figure 4e). The glacial-interglacial changes in δ^{13}C and B/Ca of *O. umbonatus* are generally consistent with δ^{13}C and B/Ca in *C. wuellerstorfi* from the subpolar North Atlantic Ocean at water depths between 2,000 and 3,000 m (Yu et al., 2008) (Figure 4). This supports the inference of Yu et al. (2008) that the Nordic Seas have contributed to the lower glacial North Atlantic intermediate water (LGNAIW) water mass. Idealized numerical modeling shows that under extensive sea-ice cover and subsurface inflow of Atlantic water into the Nordic Seas, Atlantic water recirculates as a western boundary current out of the Nordic seas (Jensen et al., 2018). The Denmark Strait may therefore have provided an overflow pathway of the subsurface Atlantic water to the North Atlantic Ocean.

3.4. Changes in the Terrestrial Carbon Input and Carbon Cycle Modeling

During the later part of Heinrich stadial 2 and the transition to interstadial 2, δ^{13}C of organic material and C/N from three nearby records show a significant and relatively abrupt decrease suggesting an increase in the input of terrestrial carbon (Hebbeln et al., 1994; see Figure 4d). This is associated with a decrease in %CaCO3 and an increase in Ice Rafted Debris (IRD) (Hebbeln et al., 1994). Although a limited number of records of δ^{13}C measured in organic material are available from the region (Hebbeln et al., 1994), the decrease in %CaCO$_3$ and increase in IRD close to the end of Heinrich stadial 2 are widely recorded from the northern Nordic Seas (e.g., Jessen et al., 2010; Zamelczyk et al., 2014) and suggest that the increase in the input of terrestrial carbon was probably a geographically wide-spread feature. This possibly hints to a mobilization event of Arctic permafrost and/or carbon release from ice sheets. Arctic permafrost, which can be divided into terrestrial (~1,000 Pg C), ice complex (~400 Pg C) and subsea (~1,400 Pg C) permafrost, is a major active component of the global carbon cycle (e.g., Tarnocai et al., 2009; Vonk et al., 2012). Also, ice sheets represent an interactive player in the global carbon cycle (e.g., Wadham et al., 2019). Within the limitation of our chronology due to uncertainty about past changes in R (Section 2.4), this event may have occurred sometime between 24.5 ka and 23 ka. We do not have constraints on the source, magnitude or transport pathways of this possible "terrestrial carbon" mobilization event. However, some of this mobilized carbon likely entered the atmosphere directly, while a smaller part entered the Arctic Ocean system.
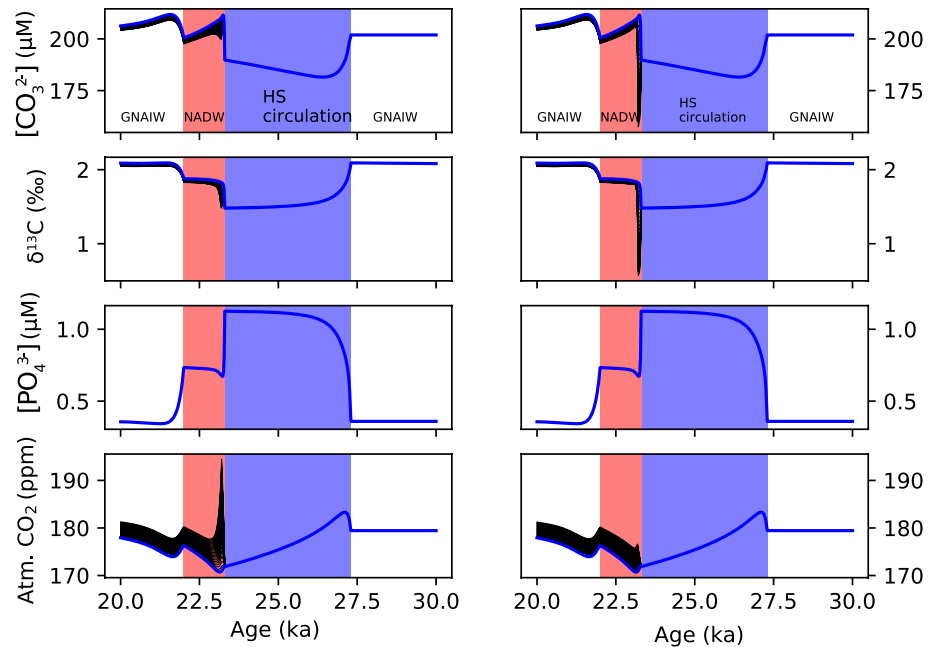
Figure 5. Modeled changes in deep "Northern Component Water" from idealized circulation changes (blue line) and carbon addition (0–88 Pg C; 1 Pg C = 1,015 gram carbon) scenarios (black lines). The model results from the "direct carbon addition to the atmosphere" and the "carbon addition to the deep North Atlantic" experiments are shown (black lines) at the left and right panels, respectively. Abbreviations: GNAIW, Glacial North Atlantic Intermediate Water; HS, Heinrich Stadial; NADW, North Atlantic Deep Water.

Although ocean biological and physical processes have likely been leading mechanisms for the glacial/interglacial and millennial-scale variations in atmospheric pCO_2, and may contribute to centennial-scale changes (e.g., Ezat et al., 2017; Rae et al., 2018), oxidation of terrestrial organic carbon may also have played a role in abrupt centennial-scale events (e.g., Bauska et al., 2016; Köhler et al., 2014; Meyer, Hefter, Köhler, Tiedemann, Gersonde, Wacker, & Mollenhauer, 2019). Given the evidence of an abrupt increase of 10 ppm in atmospheric CO_2 (e.g., Bereiter et al., 2015) and an enhanced influx of terrestrial carbon to the Nordic Seas (Hebbeln et al., 1994) at the Heinrich stadial 2/interstadial 2 transition, we are interested in finding out if and how the mobilization of terrestrial carbon in the northern high latitudes is recorded in the deep "Northern Component Water". To test the relative sensitivity of atmospheric pCO_2 and "Northern Component Water" carbonate chemistry, we superimpose two sets of carbon mobilization scenarios onto the CYCLOPS model idealized circulation scenario, with one set adding respired carbon directly to the atmosphere (Figure 5, left panel) or alternatively directly to "Northern Component Water" (Figure 5, right panel). In both cases, carbon is added for 100 years with cumulative mobilization ranging 0–88 Pg C for individual realizations. If ~45 Pg C are directly released to the atmosphere, simulated atmospheric pCO_2 experiences an abrupt and short-lived 10 ppm increase, similar to reconstructions of interstadial 2 (Figure 4g). In all cases where the carbon is added to the atmosphere the global surface ocean immediately absorbs about half of the added carbon and the associated ocean acidification and Suess effect are dispersed and not concentrated near the boreal source and "Northern Component Water". The carbonate chemistry and $\delta^{13}C$ of DIC remain principally controlled by large-scale changes in ocean circulation, and not by the carbon addition. In contrast, if the carbon is released to the "Northern Component Water", the model predicts abrupt and severe decline of $[CO_3^{2-}]$ and $\delta^{13}C$ of DIC in the "Northern Component Water" because the carbon becomes concentrated in the interior Atlantic rather than dispersed globally. For that reason carbon release to the "Northern Component Water" is unlikely to result in a transient atmospheric pCO_2 spike. It is expected that the anomalies in $[CO_3^{2-}]$ and $\delta^{13}C$ of DIC in the "Northern Component Water" depend on the rate of carbon release because with NADW circulation during interstadial 2, the water residence time in the "Northern Component Water" is short and advection and dissipation of the added carbon to the global deep ocean is facilitated by the vigorous AMOC. From these idealized carbon mobilization scenarios, we conclude that carbonate chemistry and $\delta^{13}C$ from the Nordic Seas should be relatively sensitive to respiration of terrestrial

organic matter at depth, where carbon remains relatively concentrated until ocean circulation dissipates the added carbon. This pathway of carbon mobilization has only a minimal transient effect on atmospheric pCO_2 because the carbon is initially concentrated and then dissipated within the ocean interior. The alternative pathway, direct release to the atmosphere, causes an immediate CO_2 transient that is, moderated by the global surface ocean Revelle buffer factor and its total buffer capacity, with the global dispersion of the added carbon precluding the generation of significant regionally focused carbonate chemistry anomalies. We only observe modest changes in our B/Ca and $\delta^{13}C$ records at the Heinrich stadial 2/interstadial 2 transition (Figures 4b and 4c). Thus, if the terrestrial organic matter influx at Heinrich stadial 2/interstadial 2 (Hebbeln et al., 1994, Figure 4) recorded a mobilization event of subglacial or permafrost carbon, the total carbon release was likely low or slow, or released directly to the atmosphere.

4. Conclusions

In this study, we reconstructed deep ocean hydrographic changes in the northern Nordic Seas during the late glacial (35–19 ka). Furthermore, we investigated the ambiguously large differences of $\delta^{18}O$ between two benthic foraminiferal species *Oridorsalis umbonatus* (shallow infaunal) and *Cibicidoides wuellerstorfi* (epifaunal) that have been recorded from sediments dating from the last glacial maximum (LGM) in the central and northern Nordic Seas. Using species-specific foraminiferal ^{14}C dating, we showed that the specimens of *C. wuellerstorfi* have been reworked. We therefore based our reconstructions on the most persistent and abundant benthic species *O. umbonatus*. We propose that the reconstruction of glacial ocean circulation in low-resolution deep-sea sediments from this region based on $\delta^{18}O$ and $\delta^{13}C$ measured in *C. wuellerstorfi* should be treated with caution.

Our bottom water temperatures (BWT) from Mg/Ca show, in agreement with previous studies from the Arctic Ocean and central Nordic Seas, that the deep northern Nordic Seas were on average 1.5°C warmer during the late glacial compared to the Holocene. Furthermore, local (and potentially regional) seawater $\delta^{18}O$ was 0.7 and 1‰ higher during late MIS 3 and the LGM, respectively, relative to the Holocene. The similarity in the magnitude and evolution between our seawater $\delta^{18}O$ record and global average ocean $\delta^{18}O$ supports the recent ^{14}C evidence of persistent exchange between the Arctic Ocean and the Nordic Seas and other ocean basins during the late glacial. In addition, the similar signatures of elevated $[CO_3^{2-}]$ and lower $\delta^{13}C$ during the late glacial in the subpolar North Atlantic between 2,000 and 3,000 m water depth and the northern Nordic Seas is a strong indication that the Nordic Seas may have contributed significantly to the lower glacial North Atlantic intermediate water. Altogether, our results indicate that during the late glacial the Atlantic water thickened and deepened to at least 2,600 m water depth and flowed as a subsurface intermediate layer in the Nordic Seas and the Arctic Ocean with active overflows to the North Atlantic Ocean likely via the Denmark Strait. Open ocean convection in the Nordic seas probably ceased or became intermittent.

Finally, evidence from previous studies suggests enhanced terrestrial carbon flux to the northern Nordic Seas at the Heinrich stadial/interstadial 2 transition (~23.5 ka). Comparing our $[CO_3^{2-}]$ and $\delta^{13}C$ records with carbon cycle model results, we conclude that either the total subglacial or permafrost carbon release either was low or slow, or released directly to the atmosphere.

Data Availability Statement

The new data presented in this article are available in the "Supporting Information" and will be available at Zenodo database upon acceptance of this manuscript, https://doi.org/10.5281/zenodo.4436094.

References

Ahn, J., & Brook, E. J., (2014). Siple Dome ice reveals two modes of millennial CO_2 change during the last ice age. *Nature Communications*, *5*(1), 1–6.

Bard, E., Hamelin, B., & Fairbanks, R. G. (1990). U-Th ages obtained by mass spectrometry in corals from Barbados: Sea level during the past 130,000 years. *Nature*, *346*, 456–458. https://doi.org/10.1038/346456a0

Barker, S., Cacho, I., Benway, H., & Tachikawa, K. (2005). Planktonic foraminiferal Mg/Ca as a proxy for past oceanic temperatures: A methodological overview and data compilation for the Last Glacial Maximum. *Quaternary Science Reviews*, *24*, 821–834. https://doi.org/10.1016/j.quascirev.2004.07.016

Barker, S., Knorr, G., Edwards, R. L., Parrenin, F., Putnam, A. E., Skinner, L. C., et al. (2011). 800,000 years of abrupt climate variability. *Science*, *334*, 347–351. https://doi.org/10.1126/science.1203580

Barrientos, N., Lear, C. H., Jakobsson, M., Stranne, C., O'Regan, M., Cronin, T. M., et al. (2018). Arctic Ocean benthic foraminifera Mg/Ca ratios and global Mg/Ca-temperature calibrations: New constraints at low temperatures. *Geochimica et Cosmochimica Acta*, *236*, 240–259. https://doi.org/10.1016/j.gca.2018.02.036

Bauch, H. A., Erlenkeuser, H., Spielhagen, R. F., Struck, U., Matthiessen, J., Thiede, J., & Heinemeier, J. (2001). A multiproxy reconstruction of the evolution of deep and surface waters in the subarctic Nordic seas over the last 30,000 yr. *Quaternary Science Reviews*, *20*, 659–678. https://doi.org/10.1016/s0277-3791(00)00098-6

Bauska, T. K., Baggenstos, D., Brook, E. J., Mix, A. C., Marcott, S. A., Patrenko, V. V., et al. (2016). Carbon isotopes characterize rapid changes in atmospheric carbon dioxide during the last deglaciation. *Proceedings of the National Academy of Sciences*, *113*(13), 3465–3470.

Bauska, T. K., Brook, E. J., Marcott, S. A., Baggenstos, D., Shackleton, S., Severinghaus, J. P., & Petrenko, V. V. (2018). Controls on millennial-scale atmospheric CO_2 variability during the last glacial period. *Geophysical Research Letters*, *45*, 7731–7740. https://doi.org/10.1029/2018gl077881

Bemis, B. E., Spero, H. J., Bijma, J., & Lea, D. W. (1998). Reevaluation of the oxygen isotopic composition of planktonic foraminifera: Experimental results and revised paleotemperature equations. *Paleoceanography*, *13*, 150–160. https://doi.org/10.1029/98pa00070

Bereiter, B., Eggleston, S., Schmitt, J., Nehrbass-Ahles, C., Stocker, T. F., Fischer, H., et al. (2015). Revision of the EPICA Dome C CO_2 record from 800 to 600 kyr before present. *Geophysical Research Letters*, *42*, 542–549. https://doi.org/10.1002/2014gl061957

Bjørk, A. A., Kjaer, K. H., Korsgaard, N. J., Khan, S. A., Kjeldsen, K. K., Andresen, C. S., et al. (2012). An aerial view of 80 years of climate-related glacier fluctuations in southeast Greenland. *Nature Geoscience*, *5*, 427–432.

Boyle, E. A., & Keigwin, L. D. (1985). Comparison of Atlantic and Pacific paleochemical records for the last 215,000 years: Changes in deep ocean circulation and chemical inventories. *Earth and Planetary Science Letters*, *76*, 135–150. https://doi.org/10.1016/0012-821x(85)90154-2

Broecker, W. S. (1998). Paleocean circulation during the last deglaciation: A bipolar seesaw? *Paleoceanography*, *13*, 119–121. https://doi.org/10.1029/97pa03707

Broecker, W. S., & Peng, T. H. (1982). *Tracers in the sea*.

Butzin, M., Heaton, T. J., Köhler, P., & Lohmann, G. (2020). A short note on marine reservoir age simulations used in IntCal20. *Radiocarbon*, *1–7*.

Clark, P. U., Dyke, A. S., Shakun, J. D., Carlson, A. E., Clark, J., Wohlfarth, B., et al. (2009). The last glacial maximum. *Science*, *325*, 710–714. https://doi.org/10.1126/science.1172873

Corliss, B. H. (1985). Microhabitats of benthic foraminifera within deep-sea sediments. *Nature*, *314*, 435–438. https://doi.org/10.1038/314435a0

Cronin, T. M., Dwyer, G. S., Farmer, J., Bauch, H. A., Spielhagen, R. F., Jakobsson, M., et al. (2012). Deep Arctic Ocean warming during the last glacial cycle. *Nature Geoscience*, *5*, 631–634. https://doi.org/10.1038/ngeo1557

Dansgaard, W., Johnsen, S. J., Clausen, H. B., Dahl-Jensen, D., Gundestrup, N. S., Hammer, C. U., et al. (1993). Evidence for general instability of past climate from a 250-kyr ice-core record. *Nature*, *364*, 218–220. https://doi.org/10.1038/364218a0

Duplessy, J. C., Shackleton, N. J., Fairbanks, R. G., Labeyrie, L., Oppo, D., & Kallel, N. (1988). Deepwater source variations during the last climatic cycle and their impact on the global deepwater circulation. *Paleoceanography*, *3*, 343–360. https://doi.org/10.1029/pa003i003p00343

Elderfield, H., Yu, J., Anand, P., Kiefer, T., & Nyland, B. (2006). Calibrations for benthic foraminiferal Mg/Ca paleothermometry and the carbonate ion hypothesis. *Earth and Planetary Science Letters*, *250*, 633–649. https://doi.org/10.1016/j.epsl.2006.07.041

Ezat, M. M., Rasmussen, T. L., & Groeneveld, J. (2014). Persistent intermediate water warming during cold stadials in the southeastern Nordic seas during the past 65 ky. *Geology*, *42*, 663–666. https://doi.org/10.1130/g35579.1

Ezat, M. M., Rasmussen, T. L., Hönisch, B., Groeneveld, J., & Demenocal, P. (2017). Episodic release of CO_2 from the high-latitude North Atlantic Ocean during the last 135 kyr. *Nature Communications*, *8*, 1–10. https://doi.org/10.1038/ncomms14498

Ezat, M. M., Rasmussen, T. L., Skinner, L. C., & Zamelczyk, K. (2019). Deep ocean 14C ventilation age reconstructions from the Arctic Mediterranean reassessed. *Earth and Planetary Science Letters*, *518*, 67–75. https://doi.org/10.1016/j.epsl.2019.04.027

Fischer, H., Schmitt, J., Lüthi, D., Stocker, T. F., Tschumi, T., Parekh, P., et al. (2010). The role of Southern Ocean processes on orbital and millennial CO_2 variations: A synthesis. *Quaternary Science Reviews*, *29*, 193–205. https://doi.org/10.1016/j.quascirev.2009.06.007

Gottschalk, J., Szidat, S., Michel, E., Mazaud, A., Salazar, G., Battaglia, M., et al. (2018). Radiocarbon measurements of small-size foraminiferal samples with the Mini Carbon Dating System (MICADAS) at the University of Bern: Implications for paleoclimate reconstructions. *Radiocarbon*, *60*, 469–491. https://doi.org/10.1017/rdc.2018.3

Hain, M. P., Sigman, D. M., & Haug, G. H. (2010). Carbon dioxide effects of Antarctic stratification, North Atlantic Intermediate Water formation, and subantarctic nutrient drawdown during the last ice age: Diagnosis and synthesis in a geochemical box model. *Global Biogeochemical Cycles*, *24*. https://doi.org/10.1029/2010gb003790

Hain, M. P., Sigman, D. M., & Haug, G. H. (2014). Distinct roles of the Southern Ocean and North Atlantic in the deglacial atmospheric radiocarbon decline. *Earth and Planetary Science Letters*, *394*, 198–208. https://doi.org/10.1016/j.epsl.2014.03.020

Hansen, B., & Østerhus, S. (2000). North Atlantic–Nordic seas exchanges. *Progress in Oceanography*, *45*, 109–208. https://doi.org/10.1016/s0079-6611(99)00052-x

Hanslik, D., Jakobsson, M., Backman, J., Björck, S., Sellén, E., O'Regan, M., et al. (2010). Quaternary Arctic Ocean sea ice variations and radiocarbon reservoir age corrections. *Quaternary Science Reviews*, *29*, 3430–3441. https://doi.org/10.1016/j.quascirev.2010.06.011

Heaton, T. J., Köhler, P., Butzin, M., Bard, E., Reimer, R. W., Austin, W. E. N., et al. (2020). Marine20—The marine radiocarbon age calibration curve (0–55,000 cal BP). *Radiocarbon*, *62*, 779–820. https://doi.org/10.1017/rdc.2020.68

Hebbeln, D., Dokken, T., Andersen, E. S., Hald, M., & Elverhøi, A. (1994). Moisture supply for northern ice-sheet growth during the Last Glacial Maximum. *Nature*, *370*, 357–360. https://doi.org/10.1038/370357a0

Huber, C., Leuenberger, M., Spahni, R., Flückiger, J., Schwander, J., Stocker, T. F., et al. (2006). Isotope calibrated Greenland temperature record over Marine Isotope Stage 3 and its relation to CH4. *Earth and Planetary Science Letters*, *243*, 504–519. https://doi.org/10.1016/j.epsl.2006.01.002

Jensen, M. F., Nisancioglu, K. H., & Spall, M. A. (2018). Large changes in sea ice triggered by small changes in Atlantic water temperature. *Journal of Climate*, *31*, 4847–4863. https://doi.org/10.1175/jcli-d-17-0802.1

Jessen, S. P., Rasmussen, T. L., Nielsen, T., & Solheim, A. (2010). A new Late Weichselian and Holocene marine chronology for the western Svalbard slope 30,000–0 cal years BP. *Quaternary Science Reviews*, *29*, 1301–1312. https://doi.org/10.1016/j.quascirev.2010.02.020

Knies, J., Koseoglu, D., Rise, L., Baeten, N., Bellec, V. K., Boe, R., et al. (2018). Nordic seas polynyas and their role in preconditioning marine productivity during the Last Glacial Maximum. *Nature Communications*, *9*, 1–10. https://doi.org/10.1038/s41467-018-06252-8

Köhler, P., Knorr, G., & Bard, E. (2014). Permafrost thawing as a possible source of abrupt carbon release at the onset of the Bølling/Allerød. *Nature Communications*, *5*, 1–10. https://doi.org/10.1038/ncomms6520

Köhler, P., Knorr, G., Buiron, D., Lourantou, A., & Chappellaz, J. (2011). Abrupt rise in atmospheric CO_2 at the onset of the Bølling/Allerød: In-situ ice core data versus true atmospheric signals. *Climate of the Past*, *7*(2), 473–486.

Luckman, A., Murray, T., De Lange, R., & Hanna, E. (2006). Rapid and synchronous ice-dynamic changes in East Greenland. *Geophysical Research Letters*, *33*. https://doi.org/10.1029/2005gl025428

Lynch-Stieglitz, J., Adkins, J. F., Curry, W. B., Dokken, T., Hall, I. R., Herguera, J. C., et al. (2007). Atlantic meridional overturning circulation during the Last Glacial Maximum. *Science*, *316*, 66–69.

Mackensen, A., & Schmiedl, G. (2019). Stable carbon isotopes in paleoceanography: Atmosphere, oceans, and sediments. *Earth-Science Reviews*, 102893.

Mankoff, K. D., Solgaard, A., Colgan, W., Ahlstrøm, A. P., Khan, S. A., & Fausto, R. S. (2020). Greenland Ice Sheet solid ice discharge from 1986 through March 2020. *Earth System Science Data*, *12*, 1367–1383. https://doi.org/10.5194/essd-12-1367-2020

Marchitto, T. M., Curry, W. B., Lynch-Stieglitz, J., Bryan, S. P., Cobb, K. M., & Lund, D. C. (2014). Improved oxygen isotope temperature calibrations for cosmopolitan benthic foraminifera. *Geochimica et Cosmochimica Acta*, *130*, 1–11.

Marcott, S. A., Bauska, T. K., Buizert, C., Steig, E. J., Rosen, J. L., Cuffey, K. M., et al. (2014). Centennial-scale changes in the global carbon cycle during the last deglaciation. *Nature*, *514*, 616–619. https://doi.org/10.1038/nature13799

Meyer, V. D., Hefter, J., Köhler, P., Tiedemann, R., Gersonde, R., Wacker, L., et al. (2019b). Permafrost-carbon mobilization in Beringia caused by deglacial meltwater runoff, sea-level rise and warming. In *Determination of B/Ca of natural carbonates by HR-ICP-MS* (Vol. 14, pp. 1617–1628). https://doi.org/10.1088/1748-9326/ab2653

Meyer, V. D., Hefter, J., Köhler, P., Tiedemann, R., Gersonde, R., Wacker, L., & Mollenhauer, G. (2019a). Permafrost-carbon mobilization in Beringia caused by deglacial meltwater runoff, sea-level rise and warming. *Environmental Research Letters*, *14*(8), 085003.

Misra, S., Greaves, M., Owen, R., Kerr, J., Elmore, A. C., & Elderfield, H. (2014). Determination of B/Ca of natural carbonates by HR-ICP-MS. *Geochemistry, Geophysics, Geosystems*, *15*(4), 1617–1628.

Murray, J. W. (2006). *Ecology and applications of benthic foraminifera*. Cambridge University Press.

Pena, L. D., Calvo, E., Cacho, I., Eggins, S., & Pelejero, C. (2005). Identification and removal of Mn-Mg-rich contaminant phases on foraminiferal tests: Implications for Mg/Ca past temperature reconstructions. *Geochemistry, Geophysics, Geosystems*, *6*. https://doi.org/10.1029/2005gc000930

Peng, T. H., & Broecker, W. S. (1984). The impacts of bioturbation on the age difference between benthic and planktonic foraminifera in deep sea sediments. *Nuclear Instruments and Methods in Physics Research Section B*, *5*, 346–352. https://doi.org/10.1016/0168-583x(84)90540-8

Rae, J. W., Burke, A., Robinson, L. F., Adkins, J. F., Chen, T., Cole, C., et al. (2018). CO_2 storage and release in the deep Southern Ocean on millennial to centennial timescales. *Nature*, *562*, 569–573. https://doi.org/10.1038/s41586-018-0614-0

Rae, J. W., Foster, G. L., Schmidt, D. N., & Elliott, T. (2011). Boron isotopes and B/Ca in benthic foraminifera: Proxies for the deep ocean carbonate system. *Earth and Planetary Science Letters*, *302*, 403–413. https://doi.org/10.1016/j.epsl.2010.12.034

Rasmussen, T. L., & Thomsen, E. (2004). The role of the North Atlantic Drift in the millennial timescale glacial climate fluctuations. *Palaeogeography, Palaeoclimatology, Palaeoecology*, *210*, 101–116. https://doi.org/10.1016/j.palaeo.2004.04.005

Reimer, P. J., Bard, E., Bayliss, A., Beck, J. W., Blackwell, P. G., Ramsay, C. B., et al. (2013). IntCal13 and Marine13 radiocarbon age calibration curves 0–50,000 years cal BP. *Radiocarbon*, *55*(4), 1869–1887.

Shackleton, N. J. (1974). *Attainment of isotopic equilibrium between Ocean Water and the benthonic foraminifera genus Uvigerina: Isotopic changes in the ocean during the last glacial*.

Sigman, D. M., Hain, M. P., & Haug, G. H. (2010). The polar ocean and glacial cycles in atmospheric CO_2 concentration. *Nature*, *466*, 47–55. https://doi.org/10.1038/nature09149

Sigman, D. M., Lehman, S. J., & Oppo, D. W. (2003). Evaluating mechanisms of nutrient depletion and ^{13}C enrichment in the intermediate-depth Atlantic during the last ice age. *Paleoceanography*, *18*. https://doi.org/10.1029/2002pa000818

Spratt, R. M., & Lisiecki, L. E., (2016). A Late Pleistocene sea level stack. *Climate of the Past*, *12*(4), 1079–1092.

Stuiver, M., Reimer, P. J., & Reimer, R. W. (2020). Retrieved from http://calib.org

Szidat, S., Salazar, G. A., Vogel, E., Battaglia, M., Wacker, L., Synal, H. A., & Türler, A. (2014). ^{14}C analysis and sample preparation at the new Bern Laboratory for the Analysis of Radiocarbon with AMS (LARA). *Radiocarbon*, *56*, 561–566. https://doi.org/10.2458/56.17457

Tarnocai, C., Canadell, J. G., Schuur, E. A., Kuhry, P., Mazhitova, G., & Zimov, S. (2009). Soil organic carbon pools in the northern circumpolar permafrost region. *Global Biogeochemical Cycles*, *23*. https://doi.org/10.1029/2008gb003327

Thornalley, D. J. R., Bauch, H. A., Gebbie, G., Guo, W., Ziegler, M., Bernasconi, S. M., et al. (2015). A warm and poorly ventilated deep Arctic Mediterranean during the last glacial period. *Science*, *349*, 706–710. https://doi.org/10.1126/science.aaa9554

Tisserand, A. A., Dokken, T. M., Waelbroeck, C., Gherardi, J. M., Scao, V., Fontanier, C., & Jorissen, F. (2013). Refining benthic foraminiferal Mg/Ca-temperature calibrations using core-tops from the western tropical Atlantic: Implication for paleotemperature estimation. *Geochemistry, Geophysics, Geosystems*, *14*, 929–946. https://doi.org/10.1002/ggge.20043

Veum, T., Jansen, E., Arnold, M., Beyer, I., & Duplessy, J. C. (1992). Water mass exchange between the North Atlantic and the Norwegian Sea during the past 28,000 years. *Nature*, *356*, 783–785. https://doi.org/10.1038/356783a0

Vonk, J. E., Sánchez-García, L., van Dongen, B. E., Alling, V., Kosmach, D., Charkin, A., et al. (2012). Activation of old carbon by erosion of coastal and subsea permafrost in Arctic Siberia. *Nature*, *489*, 137–140. https://doi.org/10.1038/nature11392

Wadham, J. L., Hawkings, J. R., Tarasov, L., Gregoir, L. J., Spencer, R. G. M., Gutjahr, L., et al. (2019). Ice sheets matter for the global carbon cycle. *Nature Communications*, *10*, 1–17. https://doi.org/10.1038/s41467-019-11394-4

Yu, J., Broecker, W. S., Elderfield, H., Jin, Z., McManus, J., & Zhang, F. (2010). Loss of carbon from the deep sea since the Last Glacial Maximum. *Science*, *330*, 1084–1087. https://doi.org/10.1126/science.1193221

Yu, J., & Elderfield, H. (2007). Benthic foraminiferal B/Ca ratios reflect deep water carbonate saturation state. *Earth and Planetary Science Letters*, *258*, 73–86. https://doi.org/10.1016/j.epsl.2007.03.025

Yu, J., Elderfield, H., & Piotrowski, A. M. (2008). Seawater carbonate ion-$\delta^{13}C$ systematics and application to glacial–interglacial North Atlantic Ocean circulation. *Earth and Planetary Science Letters*, *271*, 209–220. https://doi.org/10.1016/j.epsl.2008.04.010

Yu, J., Menviel, L., Jin, Z. D., Anderson, R. F., Jian, Z., Piotrowski, A. M., et al. (2020). Last glacial atmospheric CO_2 decline due to widespread Pacific deep-water expansion. *Nature Geoscience*, *13*, 628–633. https://doi.org/10.1038/s41561-020-0610-5

Yu, J., Menviel, L., Jin, Z. D., Thornalley, D. J. R., Barker, S., Marino, G., et al. (2016). Sequestration of carbon in the deep Atlantic during the last glaciation. *Nature Geoscience*, *9*, 319–324. https://doi.org/10.1038/ngeo2657

Zamelczyk, K., Rasmussen, T. L., Husum, K., Godtliebsen, F., & Hald, M. (2014). Surface water conditions and calcium carbonate preservation in the Fram Strait during marine isotope stage 2, 28.8–15.4 kyr. *Paleoceanography*, *29*, 1–12. https://doi.org/10.1002/2012pa002448